INTERFACE

rsif.royalsocietypublishing.org

Research

Cite this article: Kang BJ, Park J, Kim J, Kim HH, Lee C, Hwang JY, Lien C-L, Shung KK. 2015 High-frequency dual mode pulsed wave Doppler imaging for monitoring the functional regeneration of adult zebrafish hearts. *J. R. Soc. Interface* **12**: 20141154.
http://dx.doi.org/10.1098/rsif.2014.1154

Received: 21 October 2014
Accepted: 18 November 2014

Subject Areas:
biomedical engineering, medical physics

Keywords:
echocardiography, Doppler flow, tissue Doppler, heart regeneration, zebrafish

Author for correspondence:
Jinhyoung Park
e-mail: jinhyoung.park@gmail.com

†These authors contributed equally to this study.

Electronic supplementary material is available at http://dx.doi.org/10.1098/rsif.2014.1154 or via http://rsif.royalsocietypublishing.org.

THE ROYAL SOCIETY PUBLISHING

High-frequency dual mode pulsed wave Doppler imaging for monitoring the functional regeneration of adult zebrafish hearts

Bong Jin Kang[1,†], Jinhyoung Park[1,†], Jieun Kim[3], Hyung Ham Kim[1], Changyang Lee[1], Jae Youn Hwang[2], Ching-Ling Lien[3] and K. Kirk Shung[1]

[1]NIH Resource on Medical Ultrasonic Transducer Technology, Department of Biomedical Engineering, University of Southern California, Los Angeles, CA 90089, USA
[2]Department of Information and Communication Engineering, Daegu Gyeongbuk Institute of Science and Technology, Daegu, South Korea
[3]Saban Research Institute, Children's Hospital Los Angeles, Los Angeles, CA 90027, USA

Adult zebrafish is a well-known small animal model for studying heart regeneration. Although the regeneration of scars made by resecting the ventricular apex has been visualized with histological methods, there is no adequate imaging tool for tracking the functional recovery of the damaged heart. For this reason, high-frequency Doppler echocardiography using dual mode pulsed wave Doppler, which provides both tissue Doppler (TD) and Doppler flow in a same cardiac cycle, is developed with a 30 MHz high-frequency array ultrasound imaging system. Phantom studies show that the Doppler flow mode of the dual mode is capable of measuring the flow velocity from 0.1 to 15 cm s^{-1} with high accuracy (p-value $= 0.974 > 0.05$). In the *in vivo* study of zebrafish, both TD and Doppler flow signals were simultaneously obtained from the zebrafish heart for the first time, and the synchronized valve motions with the blood flow signals were identified. In the longitudinal study on the zebrafish heart regeneration, the parameters for diagnosing the diastolic dysfunction, for example, $E/Em < 10$, $E/A < 0.14$ for wild-type zebrafish, were measured, and the type of diastolic dysfunction caused by the amputation was found to be similar to the restrictive filling. The diastolic function was fully recovered within four weeks post-amputation.

1. Introduction

Zebrafish has been used as a small animal model to study human heart diseases owing to its fully sequenced genome [1,2] and regenerative capability [3]. After 20% of its ventricular apex is amputated, fibrin clots are formed to block the haemorrhage followed by regeneration of the damaged myocardium [4]. Those morphological recoveries are well identified through the histology of sacrificed fish hearts.

Functional recoveries were investigated by measuring either the electrical conduction of myocardium or the haemodynamics of the fish hearts. A recent study that used optical voltage mapping technique to measure the surface potential distributions of the injured zebrafish hearts found that the repolarization on the wound site was recovered within two to four weeks post-injury [5]. However, this approach requires isolation of the heart from the sacrificed fish, which limits further follow-up. In a non-invasive method, a novel zebrafish electrocardiogram (ECG) was developed to assess the extension of drug-induced QT intervals, which further implied changes in ventricular repolarization [6]. During the measurement, ECG recordings were conducted outside of the aqueous environment requiring a perfusion system for preventing hypoxia, and the zebrafish was paralysed with a sodium channel blocker to suppress gill motion. However, this method is limited in that it is unclear whether the findings are the result of the

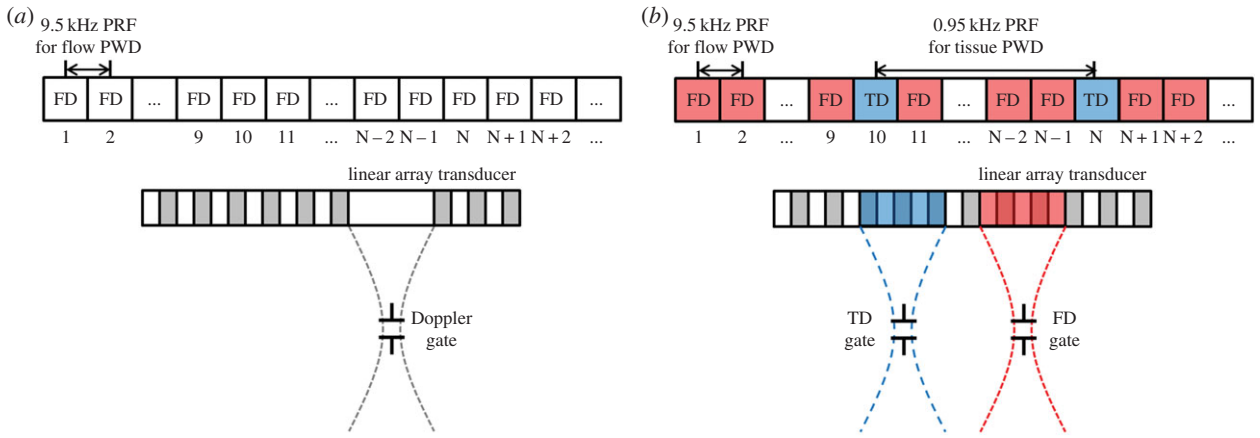

Figure 1. Beam sequences of implemented PWD: (*a*) single mode PWD and (*b*) dual mode PWD. The location of the gates for the dual mode PWD can be located at different lateral and axial positions from each other. FD is Doppler flow and TD is tissue Doppler. (Online version in colour.)

injury or from the side effects caused by the gill-motion suppression treatments. In other studies, Doppler echocardiography has been employed for non-invasive measurement of parameters directly related to haemodynamics. Blood flow in zebrafish hearts was investigated with a low-frequency (7 and 8.5 MHz) ultrasound array imaging system. Its diastolic functions were assessed by measuring the slopes of the rising or falling edge of the Doppler waveforms, generated by the early diastolic blood flow under varying ambient temperature [7]. However, the size of the Doppler gate was too large (greater than 400 µm) relative to that of the fish heart (approx. 1 mm), rendering it very difficult to measure flow signals from a specific location within the zebrafish heart. In another study using a high-frequency (45 MHz) ultrasound imaging system, flow signals in specific regions such as bulbus arteriosus, ventricle and atrium were detected; however, the measurement of flow itself did not provide adequate information for assessing the functional recovery of the fish hearts [8].

In medical ultrasound imaging, both tissue Doppler (TD) and Doppler flow modes have been employed for diagnosing human cardiac dysfunction [9]. While ventricular systolic dysfunction can be assessed by measuring the stroke volume and myocardial performance index (MPI), diastolic dysfunction can be assessed by measuring the ratio (E/A) of the peak velocities of early and late diastolic flow (E and A, respectively), the ratio (E/Em or E/E') of E and the peak velocities of early diastolic myocardial relaxation velocity (Em or E') [10]. Note that the lower-case 'm' for myocardial (Em) and the superscripted prime symbol (E') are used to differentiate TD from Doppler flow. The zebrafish heart diastolic dysfunction, resulting from heart injuries, may also be diagnosed with the same parameters used for human hearts. However, TD of zebrafish hearts has not been reported to the best of our knowledge, and the synchronization between TD and Doppler flow is challenging for investigating heart dysfunctions with arrhythmia.

In this paper, a novel method of dual mode pulsed wave Doppler (PWD) imaging, which acquires both TD and Doppler flow signals at the same time, is reported. The proposed method is developed and implemented in a high-frequency (30 MHz) linear array imaging system. TD beams, transmitted at lower pulse repetition frequency (PRF) than that of Doppler flow, are interspersed among the Doppler flow beam sequences. The performance of the dual mode PWD was validated using flow and moving wire phantoms which were designed to generate the regulated flow and the motion patterns. Adult zebrafish with amputated hearts were prepared, and longitudinal studies were conducted to observe the functional recoveries during heart regeneration. The nature of diastolic dysfunction was diagnosed by analysing the parameters associated with both Doppler flow and TD signals, and the functional recoveries of the amputated zebrafish hearts were observed.

2. Principles and implementation

2.1. Single mode pulsed wave Doppler

In single mode PWD, blood flow signals are detected by transmitting multi-cycle bursts at a PRF to where the Doppler gate is located. Here, PRF is decided by the target's maximum velocity, calculated with the following equation

$$\mathrm{PRF}_{\max} = \frac{4 v_{\max} f_0 \cos\theta}{c}, \tag{2.1}$$

where $v_{\max}$ is the maximum velocity of imaging targets, f_0 is the centre frequency of transmits, θ is the angle between the flow and the ultrasound beam, and c is the speed of sound (1540 m s^{-1}). Figure 1*a* depicts the implemented Doppler sequences at 9.5 kHz PRF. The received echo signals are demodulated into in-phase and quadrature (IQ) signals, and wall filters are applied to remove tissue clutters. The filtered signals are Fourier transformed, and the result forms a Doppler scanline [11]. Note that the Doppler shift frequency is converted into velocity using the following equation [12]

$$v = \frac{\Delta f}{2 f_0 \cos\theta} c, \tag{2.2}$$

where Δf is the measured Doppler shift frequency and f_0 is the centre frequency of the transducer.

2.2. Dual mode pulsed wave Doppler

The proposed dual mode PWD has two gates that can be located at different locations within the B-mode field of view. One gate is used to detect the blood flow signals and the other for tissue movements. Because the velocity of blood flow is faster than that of tissue movements, PRF for flow Doppler (FD) is set 10 times higher than that of TD. Dual mode PWD is implemented by interleaving TD with FD

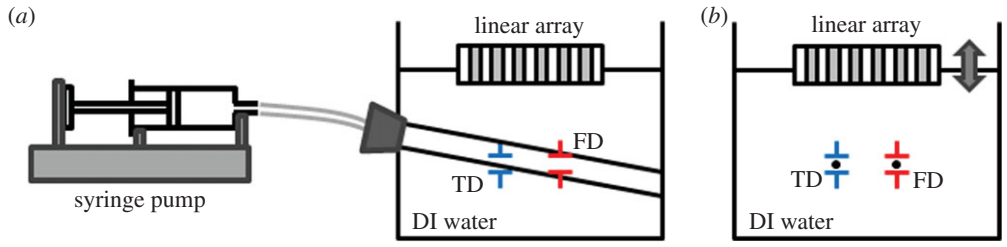

Figure 2. Experiment set-up for (*a*) flow phantom and (*b*) moving wire phantom. The flow phantom is composed of a polyimide tube with an inner diameter of 510 μm, and flow velocity is controlled by a syringe pump. The moving wire phantom is composed of two tungsten wires of 20 μm in diameter. Black dots within the Doppler gates are representing the cross sections of wire targets. (Online version in colour.)

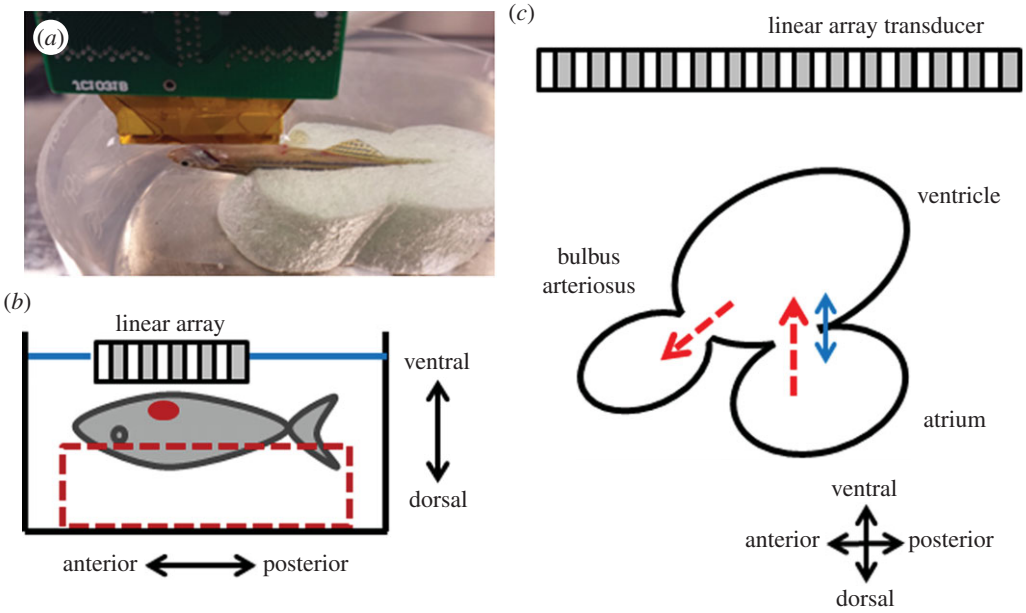

Figure 3. (*a*) The picture and (*b*) the diagram of the experimental set-up for zebrafish heart imaging. The adult zebrafish was sedated and placed on a chasm with the ventral side facing upwards and the ultrasound array was positioned above the heart. (*c*) Simplified schematic diagram of the zebrafish heart illustrates the atrium, ventricle and bulbus arteriosus. The red-dashed arrows indicate the direction of blood flow and the blue-solid arrow indicates the direction of tissue movement. (Online version in colour.)

sequences as shown in figure 1*b*, where TD sequence with a lower PRF replaces FD sequences. During the FD sequences, a Doppler flow acquisition corresponding to the TD sequence is replaced by a vector for TD instead of FD.

The missing flow vectors, caused by interleaved tissue PWD sequences, are estimated by averaging the neighbouring echoes before and after the missing vector. As illustrated in figure 1*b*, the missing flow vector in Nth sequence is estimated by averaging the echoes corresponding to the sequences of $N-2$, $N-1$, $N+1$ and $N+2$. The echo signals corresponding to the flow and the tissue PWD are separated from the acquired data for each Doppler processing.

3. Experimental arrangement

3.1. System set-up

Dual mode PWD was implemented with a custom-designed 64-channel high-frequency ultrasound imaging system [13] operating a 30 MHz linear array transducer with 256 elements [14]. Electronically focused beams were transmitted to the Doppler gate, and the returned echo signals were digitized with a sampling frequency of 120 MHz. The digitized data were beamformed and stored for further offline Doppler processing using a custom-made Matlab (Matlab 2011b, MathWorks, MA) program provided as electronic supplemental material.

3.2. Phantom study

For the quantitative evaluation of the implemented dual mode PWD, studies on flow and moving wire phantoms were performed. The flow phantom having a polyimide tube with an inner diameter of 510 μm was fabricated to evaluate the performance of measuring flow velocities. The blood-mimicking fluid prepared by mixing silicon dioxide particles in DI water was injected into the tube, and the flow velocity was controlled by a syringe pump (NE-1000 Multi-Phaser, New Era Pump System Inc., NY). Under the guidance of B-mode imaging, the gate for Doppler flow measurement was placed inside the tube, and the TD gate was placed at the wall of the polyimide tube as illustrated in figure 2*a*. The PRFs of flow and tissue PWD were set to be 9.5 kHz and 950 Hz which could detect the maximum velocities of 25.5 and 2.55 cm s^{-1} with the measured Doppler angle of 61.4°, respectively. Four different flow velocities, 3, 5, 10 and 15 cm s^{-1}, were generated using the syringe pump.

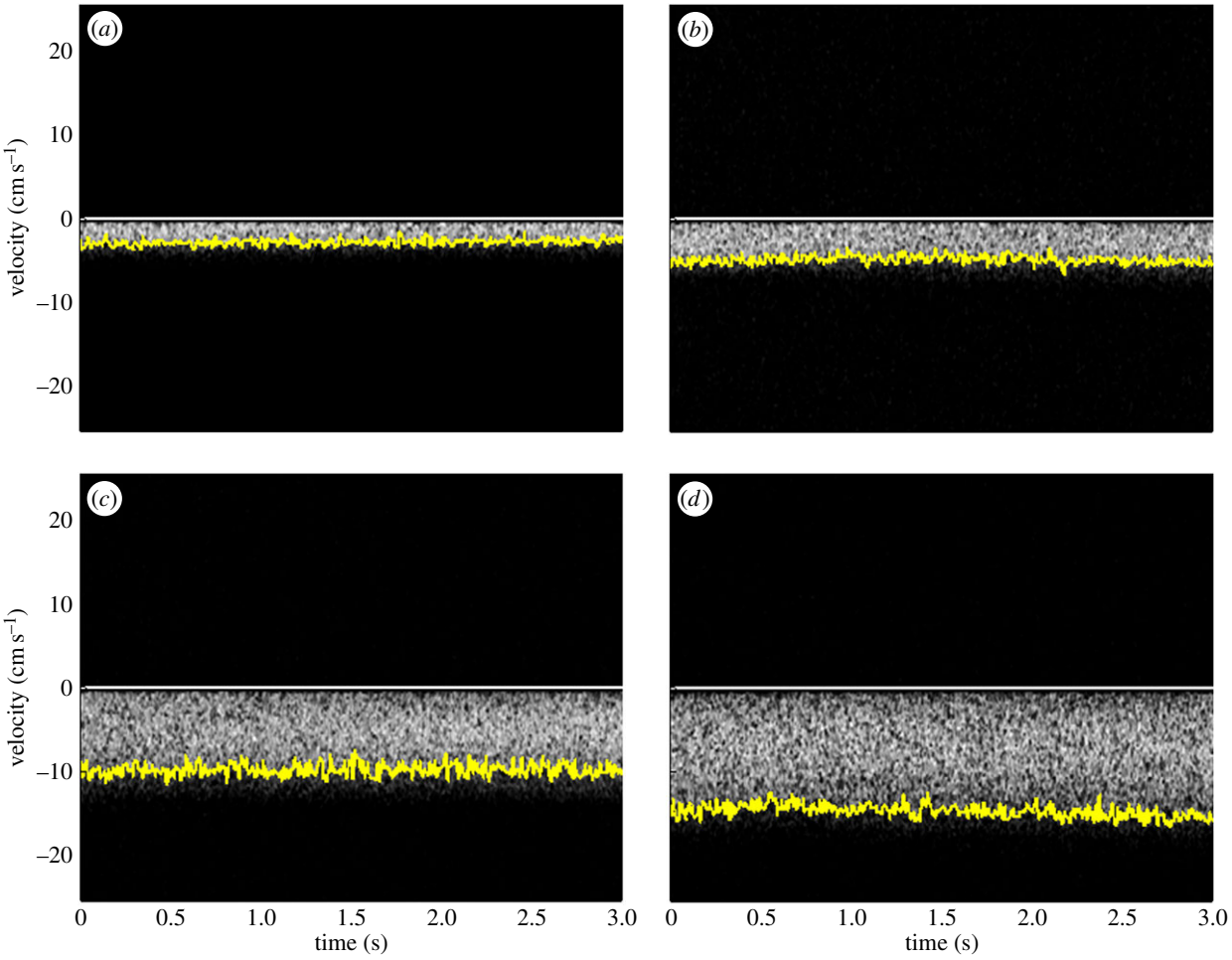

Figure 4. Doppler flow waveforms of the dual mode PWD acquired from the flow phantom with the pre-set flow velocities of (*a*) 3, (*b*) 5, (*c*) 10 and (*d*) 15 cm s^{-1}. The measured mean peak velocities are (*a*) 2.9 $\pm$ 0.37, (*b*) 4.9 $\pm$ 0.47, (*c*) 9.9 $\pm$ 0.72 and (*d*) 14.9 $\pm$ 0.77 cm s^{-1}. The yellow-solid lines indicate the maximum velocity at each moment. (Online version in colour.)

The same flow phantom was used to simulate the Doppler aliasing artefact caused by the flow speed exceeding the upper detectable velocity. While constant flow was generated and flowed through the tube, one side of the tube was clamped and released by a clip manually to disturb the flow so as to mimic the pulsatile stream. For this experiment, single mode PWD was used to acquire Doppler signals, and the echo signals corresponding to TD sequences were replaced with a vector calculated by averaging the neighbouring echoes before and after the TD sequences.

The performance of TD was evaluated by using a custom-designed moving wire phantom. The phantom having two tungsten wires of 20 µm in diameter was placed in a container filled with DI water. The transducer was mounted on a motorized three-axis stage (SGSP 20, Sigma KOKI Co., Japan), and its surface was positioned above the wire targets as shown in figure 2*b*, where the black dots within the Doppler gates denote the cross sections of wire targets. The locations of each Doppler gate in depth were fixed at the transducer's transmit focal point of 6.4 mm, and the distance between two Doppler gates in lateral direction was set at 500 µm, equal to the distance between two wires. The transducer was translated up and down at a speed of 1 mm s^{-1} to make the Doppler gates move across the wire targets instead of moving the wires. The PRFs for flow and TD were set to be 9.5 kHz and 950 Hz, respectively.

3.3. Adult zebrafish heart Doppler imaging

All adult zebrafish experiments were performed in accordance with protocols approved by the Institutional Animal Care and Use Committee at the University of Southern California. Zebrafish heart Doppler imaging was performed one week prior to ventricular amputation and 3, 7, 14, 21 and 32 days post-amputation (dpa) to monitor functional changes of the heart during regeneration process. A total of five adult zebrafish were studied and their mean body size (length) was 40.8 $\pm$ 3.6 mm (mean $\pm$ s.d.). The zebrafish was anaesthetized for 30 s by submerging it in 0.08% tricaine solution (MS-222, Sigma-Aldrich, MO) followed by removing scales around the zebrafish heart. The fish was then put into a chasm on one side of a soft sponge to fix its position of ventral side facing upwards as shown in figure 3*a*,*b*, whereas the other side was attached to the bottom of a water chamber with a double-sided tape. The chamber was filled with 0.04% tricaine solution to perform ultrasound imaging under anaesthesia at room temperature of 26°C. Using B-mode imaging to display the fish's sagittal plane of the heart which shows the largest cross section, the fish was repositioned to place one Doppler gate at the entrance of bulbus arteriosus in between the ventricular outflow tract (VOT) and the atrioventricular valve, and the other at the atrioventricular valve for detecting the flow and TD signals, respectively. The position of the zebrafish heart was adjusted to make the direction of atrioventricular blood

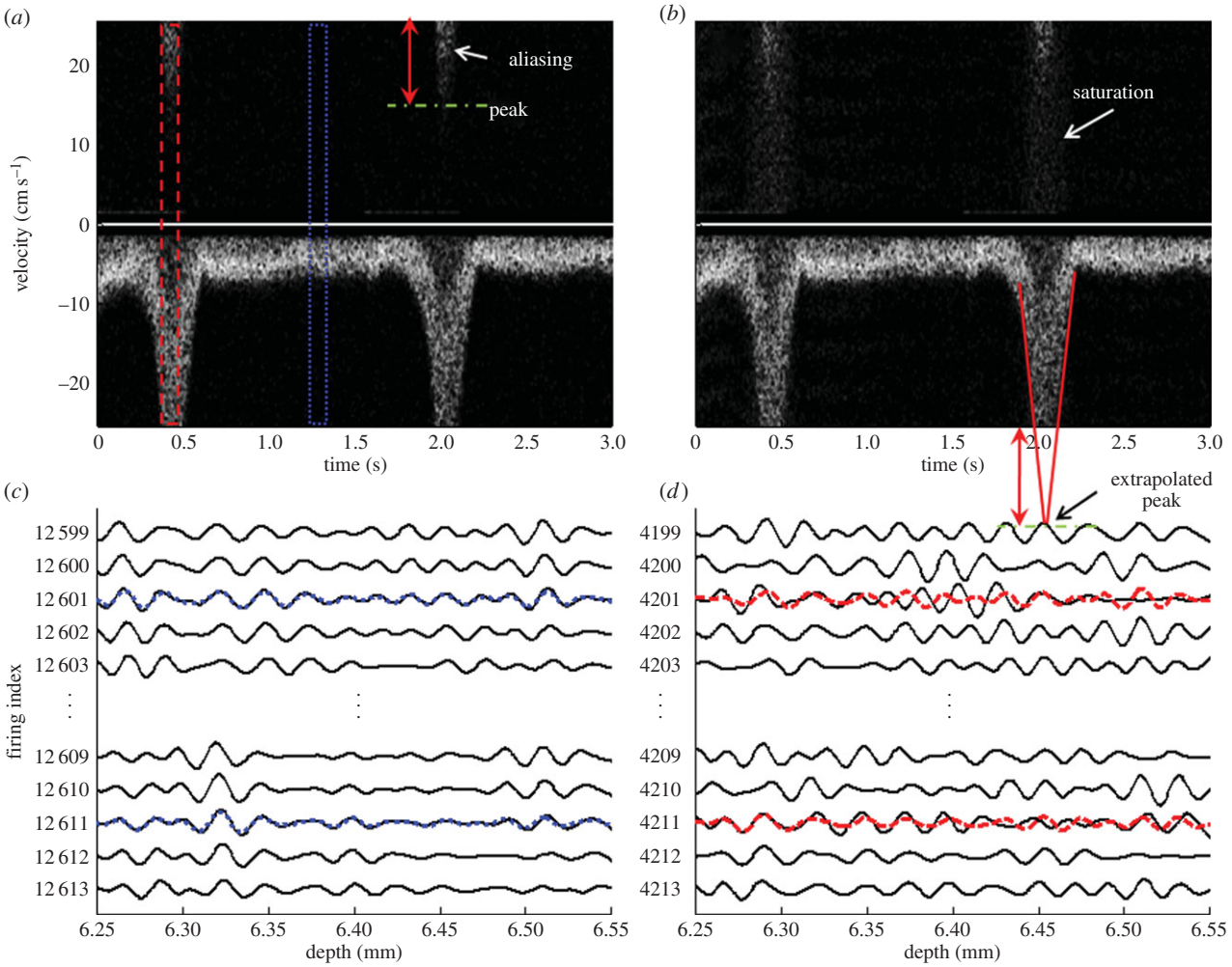

Figure 5. Doppler flow waveforms with aliasing artefacts. Doppler waveform generated by (*a*) single mode PWD and (*b*) dual mode PWD. Raw echo signals in the range of (*c*) non-aliased and (*d*) aliased region, which are represented as a blue-dotted and red-dashed line, respectively. Black-solid lines represent the raw echo signals acquired by the single mode PWD. Red-dashed and blue-dotted lines represent the reconstructed signals of the aliased and the non-aliased calculated by interpolating the neighbouring vectors. (Online version in colour.)

flow perpendicular to the transducer's surface which was parallel to the valve. Therefore, the estimated Doppler angle for detecting the atrioventricular flow was 0°. PRFs for flow and tissue PWD were set as 9.5 kHz and 950 Hz, respectively. After the gates were located, the B-mode was frozen, and Doppler data acquired in real time and post-processed by a custom-designed Matlab software.

3.4. Parameters for assessing diastolic dysfunction

Zebrafish hearts, like the human's, circulate blood with cyclic systolic and diastolic phases which are performed by the contractions and relaxations of heart muscles. In human myocardial injuries or diseases, abnormalities on the heart cycles have been observed by using parametric analysis of ultrasonic Doppler imaging method. The zebrafish diastolic dysfunction caused by the ventricular amputation may also be diagnosed and classified as one of subtypes of the diastolic dysfunction, for example, impaired relaxation, pseudo-normal and restrictive filling by using the parameters of Doppler flow and TD echocardiography [9]. To assess overall heart performance, MPI, defined by the equation below, is employed [15]:

$$\mathrm{MPI} = \frac{\mathrm{IVCT} + \mathrm{IVRT}}{\mathrm{ET}}, \tag{3.1}$$

where ET is the ejection time during the systolic phase, IVCT is the isovolumic contraction time for ventricular muscles to prepare for the flow ejection to the aorta and IVRT is the isovolumic relaxation time for reducing the ventricular pressure, which is caused by early passively filling blood flow (E-flow) from the atrium. Here, IVRT is variable depending on the compliance of the ventricular wall and affected by the damaged ventricle which causes changes in its stiffness and diastolic functions. In monitoring the velocity of heart dynamics, *E*, *A* and *E*/*A* are used to assess blood flow circulation and *E*m for monitoring tissue motion at atrioventricular valve. *E*m is reported to be related to the ventricular relaxation time, and *E*/*E*m represents the pressure gradient between the atrium and the ventricle. In previous studies on zebrafish echocardiography [7], E-flow, A-flow and ejection flow were identified, and the sequences of these flows were shown to be similar to the flow patterns observed in the human heart, although the range of these parametric values between human and zebrafish are different owing to the structural differences of the hearts, for example number of chambers, size. In addition, the patterns of zebrafish electrocardiography exhibit the same patterns of PQRST as those of the human heart, indicating that both types of hearts have comparable contractional and relational operations. Therefore, parameter change patterns caused by the damages and recoveries of the zebrafish hearts may be

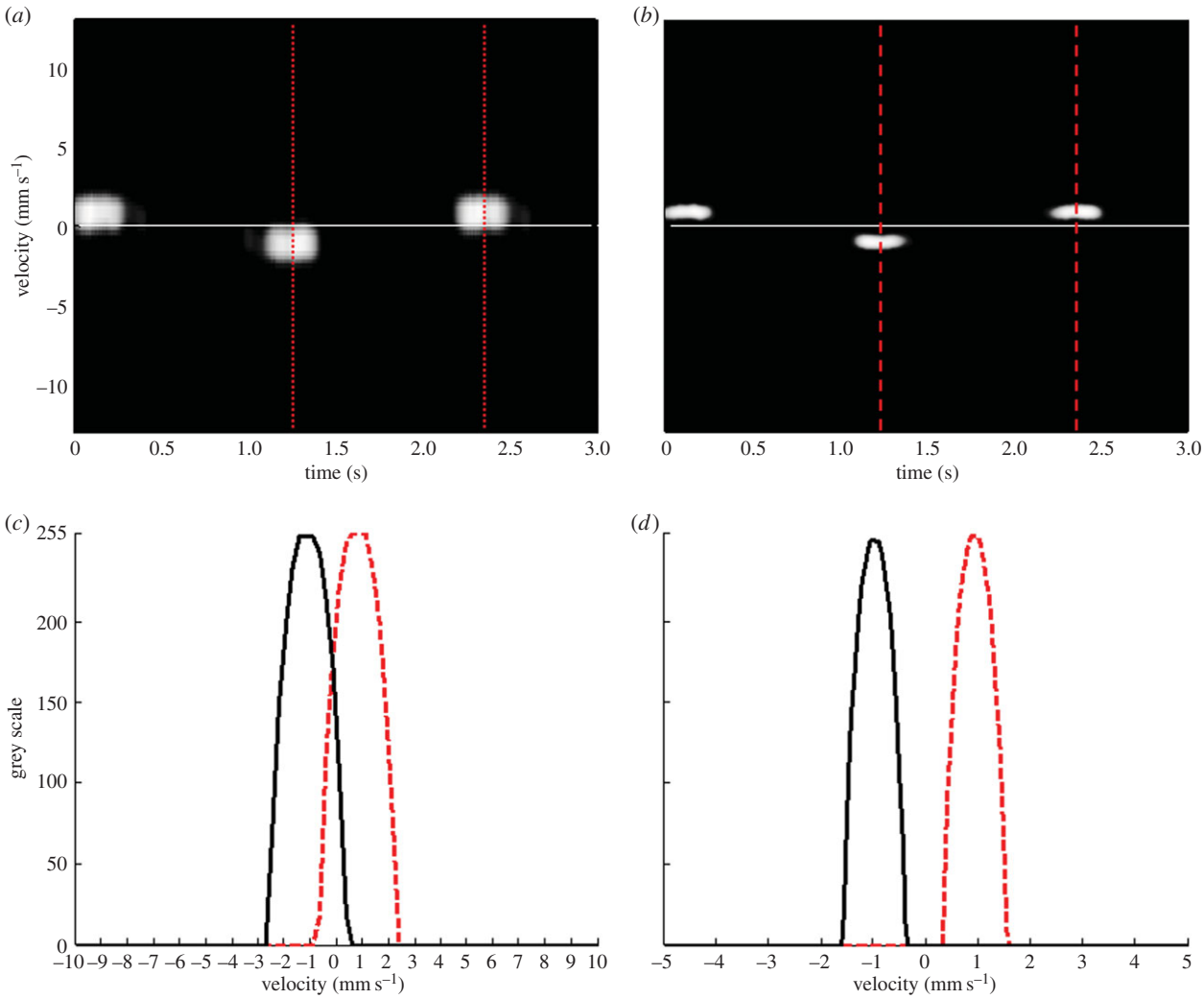

Figure 6. Doppler waveforms acquired from the moving wire phantom using the dual mode PWD: (*a*) Doppler flow image, (*b*) tissue Doppler image. Doppler intensity profiles as a function of velocities of (*c*) Doppler flow and (*d*) TD signals. Note that red-dotted and black-solid lines in (*c*) and (*d*) indicate the velocity profiles of wires moving toward and away the transducer, respectively. (Online version in colour.)

similar to those of human hearts. Based on this assumption, the Doppler parameters used to diagnose human hearts were used to evaluate the functional recovery of the amputated zebrafish heart. These parameters were measured in zebrafish hearts for 32 dpa. The relevance of comparisons between the data before and after the amputation was evaluated by the two-sided paired *t*-test, with the level of significance set at the *p*-value ≤ 0.05.

4. Results

4.1. Phantom study results

Figure 4*a–d* shows FD waveforms of dual mode PWD acquired from the flow phantom with the pre-set flow velocity of 3, 5, 10 and 15 cm s^{-1}. The yellow solid lines on the boundary of each FD image indicate the maximum velocity at each moment. The averaged velocities of each setting over 3 s are -2.9 ± 0.37, -4.9 ± 0.47, -9.9 ± 0.72 and -14.9 ± 0.77 cm s^{-1}, respectively. Note that the negative velocity indicates that the direction of the flow is away from the transducer. The maximum detectable velocity is 25.5 cm s^{-1} calculated with the PRF of 9.5 kHz and the Doppler angle of 61.4°.

Figure 5 shows the flow signals containing aliasing artefacts and compares Doppler waveforms acquired with the single mode PWD and the dual mode PWD in figure 5*a* and *b*, respectively. The signal, sharply decreasing to less than -25.5 cm s^{-1}, is aliased over the positive signal region for the single mode PWD in figure 5*a*, whereas the aliased signal in the dual mode PWD causes saturation over the whole velocity range as shown in figure 5*b*. The saturation artefacts are caused by the reconstruction of the missing FD vector replaced by the TD vector of the aliased signals. Figure 5*c*,*d* shows raw echo signals in the range of non-aliased and aliased region, shown in blue-dotted and red-dashed boxes in figure 5*a*, respectively. In figure 5*c*,*d*, black-solid lines represent the echo signals acquired with the single mode PWD, and blue-dotted and red-dashed lines indicate the interpolated signals reconstructed by averaging the neighbouring echo signals. When the signals are aliased, the neighboured vectors are decorrelated, and the original signals shown in black solid lines are not recovered with the linear interpolation method. Note that the zero lag cross-correlation coefficient between the original and the reconstructed echo signal, which represents the similarity of two signals, is 0.963 in the non-aliased region and 0.6804 in the aliased region.

Figure 6*a*,*b* shows Doppler flow and TD waveforms of the dual mode PWD acquired from the moving wire targets at a

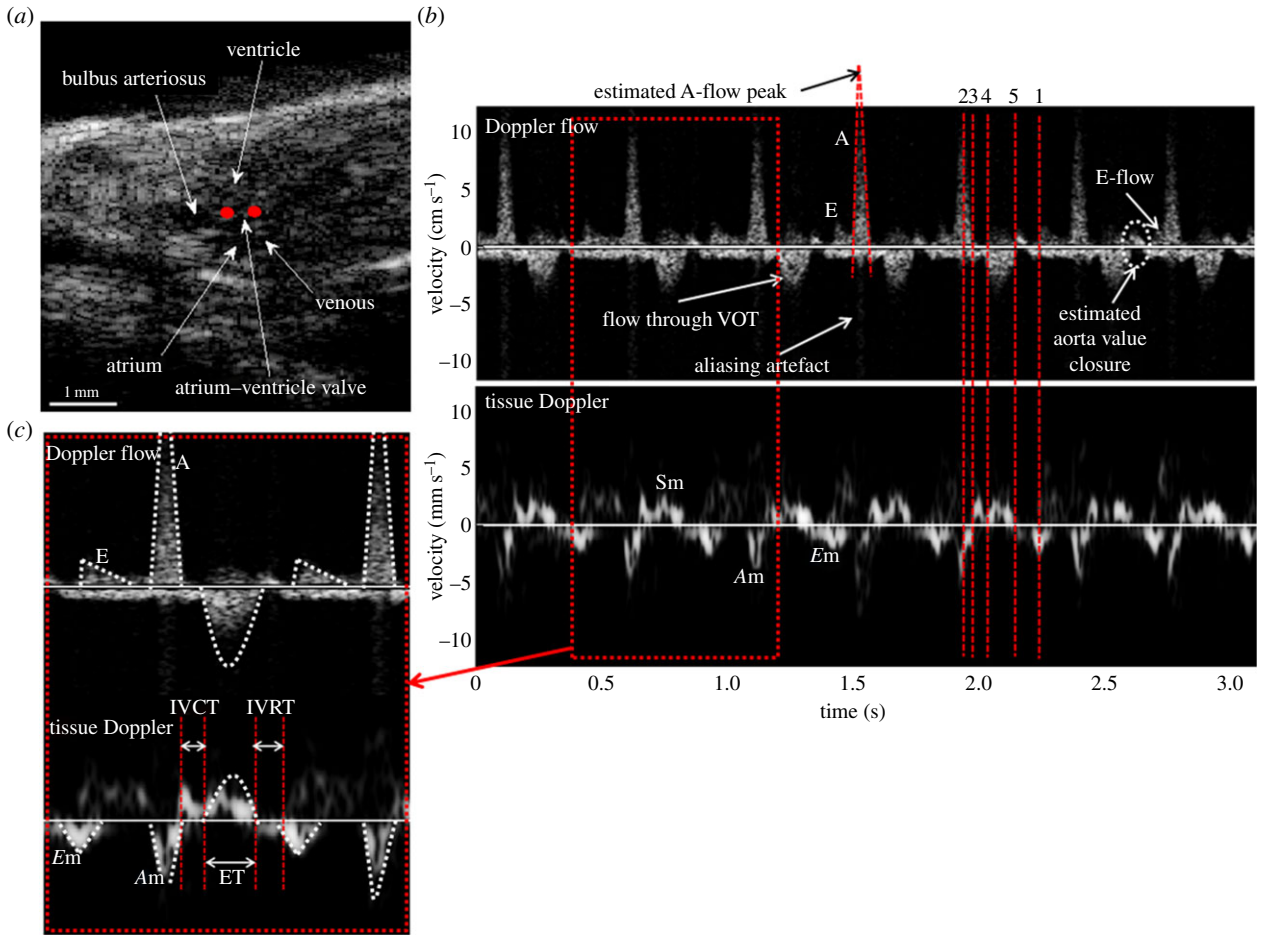

Figure 7. B-mode image and Doppler waveforms acquired with the dual mode PWD from a wild-type adult zebrafish before the heart amputation: (*a*) B-mode image of zebrafish heart in sagittal plane, (*b*) Doppler flow and tissue Doppler waveforms and (*c*) the magnified Doppler signals. The scales of the velocity are cm s^{-1} and mm s^{-1} for the Doppler flow and the TD signals, respectively. Red dots in (*a*) indicate the location of Doppler gates of the dual mode PWD. A-flow, E-flow and outflow in Doppler flow and the respective pairs of *A*m, *E*m and *S*m in TD are identified at the same moments and indicated by red-dotted lines. The time duration between the red-dashed lines of '5' and '1' represents for IVRT, '3' and '4' for IVCT, and '4' and '5' is for ET. (Online version in colour.)

speed of 1 mm s^{-1}, respectively. Figure 6*c*,*d* shows the intensity profiles as a function of velocity for the Doppler flow and TD signals, respectively. The centre velocities of both Doppler methods are measured at 1 mm s^{-1}, equal to the speed of the wire target movement. Note that the velocity range of the wire target movement in the FD is broader than the TD signal, because the same number of Doppler samples is used for both methods, whereas the resolution, pixels per unit velocity, of the FD is reduced by 10 times in comparison to the TD.

4.2. Zebrafish heart results

Figure 7*a* is the B-mode image of an adult zebrafish in the sagittal plane visualizing the whole heart, from which the structures of the heart can be identified. Under the guidance of B-mode imaging, the Doppler gates of the dual mode PWD were placed at the entrance of bulbus arteriosus and at the atrioventricular valve as marked with red dots for detecting flow and tissue signals, respectively. Figure 7*b* shows dual mode PWD signals acquired from an adult zebrafish heart showing both blood flows and tissue movements. The peak velocity of A-flow which is greater than the maximum detectable range causes the aliasing artefact, similar to the result demonstrated in the phantom study. In the presence of A-flow aliasing, the peak is estimated by drawing the lines along the outer boundaries on either side of A-FD signal and extrapolating [9]. The shape of TD pattern is also similar to that of the human heart except for the reversed velocity level of *E*m and *A*m, also evidenced in the FD pattern. The measured MPI, *E*, *A*, *E*m, *E*/*A* and *E*/*E*m values for five normal zebrafish are 0.90 ± 0.10, 1.84 ± 0.69, 15.21 ± 2.94, 2.21 ± 0.77, 0.12 ± 0.04 and 8.8 ± 3.6 mm s^{-1}, respectively, whereas the values for humans are 0.42 ± 0.09, 69 ± 12, 51 ± 11, 10 ± 3, 1.40 ± 0.36 and 5.61 ± 1.38 cm s^{-1}, respectively [9]. The notable differences in zebrafish parameters compared with those of humans are *E*/*A*, which is lower than 1 and MPI, which is higher than 0.5. The increased MPI, caused by the prolongation of IVRT, and reduced *E*/*A* are expressed in patients with impaired relaxation of diastolic dysfunction caused by lowered left ventricular compliance. Based on the observation from this study, the compliance of zebrafish heart ventricle may be lower than that of human hearts, but further investigations are required.

Using the dual mode Doppler waveforms acquired from five zebrafish, the parameters for diagnosing diastolic dysfunction are measured. The values measured on the day before amputation, 3, 7, 14, 21 and 32 dpa are indicated by diamond markers in the plots shown in figures 8 and 9, where error bars represent standard deviations. In figure 8, MPI, IVRT and IVCT are plotted. The MPI before amputation

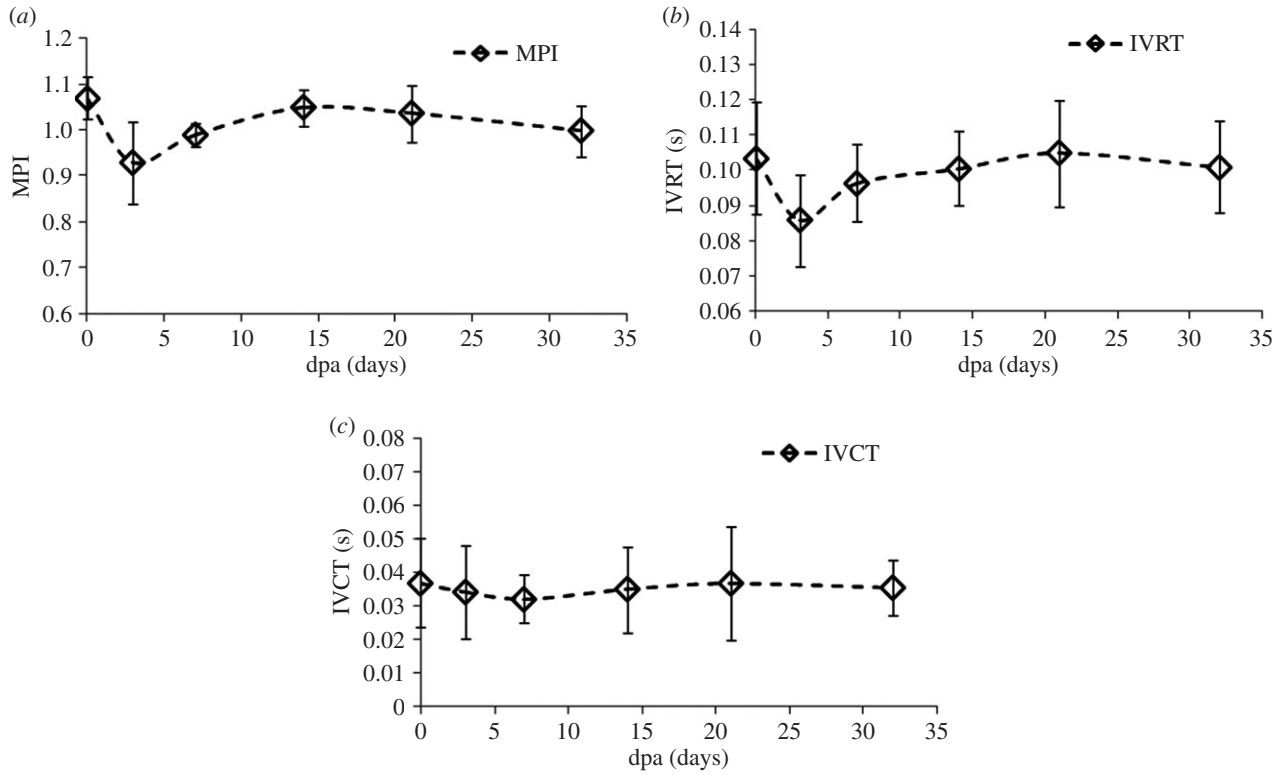

Figure 8. Amputation injury induced changes in parameters of (*a*) MPI, (*b*) IVRT and (*c*) IVCT measured in the longitudinal study. (*a*) MPI decreased at 3 dpa in comparison with MPI at 0 dpa ($p = 0.012 < 0.05$). (*b*) IVRT also decreased from 0.10 to 0.08 at 3 dpa ($p = 0.01 < 0.05$) and then returns to 0.10 at 14 dpa. (*c*) IVCT does not change significantly.

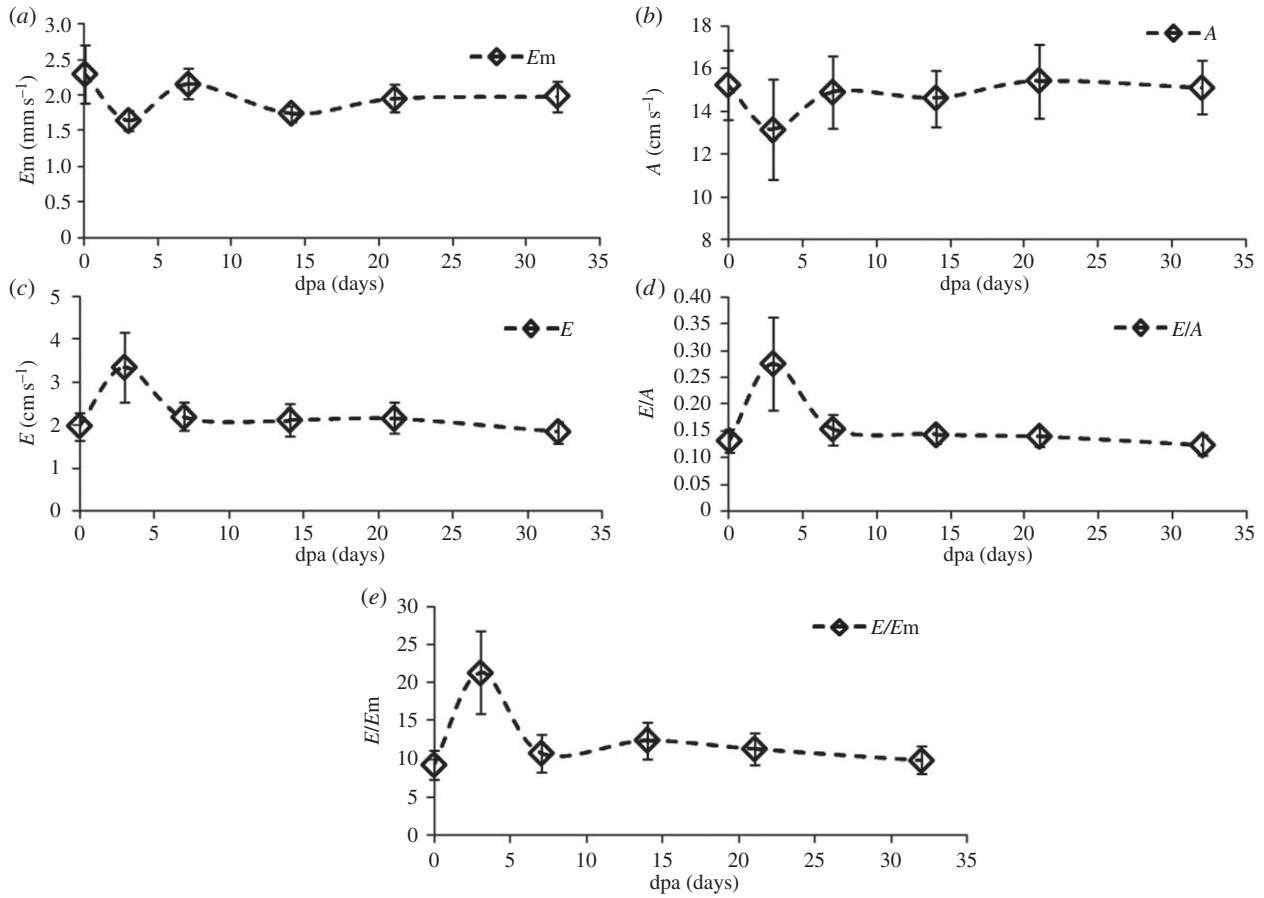

Figure 9. Amputation injury induced changes in parameters related to flow and tissue velocities: (*a*) *E*m, (*b*) *A*, (*c*) *E*, (*d*) *E*/*A*, (*e*) *E*/*E*m measured in the longitudinal study. Both *E*/*A* and *E*/*E*m increased at 3 dpa and recover to the value before amputation at 21 and 32 dpa, respectively.

is 1.07 and decreases to 0.93 at 3 dpa which is significantly different (p-value $= 0.01 < 0.05$) from the original value, whereas the MPI returns to the value before amputation by 14 dpa (p-value $= 0.66 > 0.05$). In addition, IVRT decreases from 0.10 to 0.08 at 3 dpa (p-value $= 0.01 < 0.05$) and returns to 0.10 at 14 dpa (p-value $= 0.6 > 0.05$), whereas IVCT does not show significant changes caused by the amputation (p-value $= 0.26 > 0.05$) on the day of or thereafter.

Figure 9 shows the parameters related to the tissue and blood flow dynamics. The average value of Em is significantly decreased from 2.4 to 1.6 mm s^{-1} (p-value $= 0.03 < 0.05$) and recovers at 7 dpa (p-value $= 0.33 > 0.05$). The mean value of A decreases from 14 to 11 cm s^{-1} (p-value $= 0.03 < 0.05$) and recovers at 7 dpa to 14 cm s^{-1} (p-value $= 0.85 > 0.05$). The mean value of E increases from 1.87 to 2.88 cm s^{-1} (p-value $= 0.06 > 0.05$) and returns almost to the original value at 7 dpa (p-value $= 0.56 > 0.05$). As a result, both E/A (p-value $= 0.04 < 0.05$) and E/Em (p-value $= 0.04 < 0.05$) increase at 3 dpa and recover to the pre-amputation values by 14 dpa (p-value $= 0.53 > 0.05$) and 7 dpa (p-value $= 0.58 > 0.05$), respectively.

5. Discussion

Conventional Doppler techniques using focused ultrasound beams use a single gate for detecting flow or tissue movement velocities independently. It is impossible to measure both TD and Doppler flow signals of a diseased heart in the same cardiac cycle using this method. In this study, it is demonstrated that the dual mode Doppler technique is capable of overcoming such limitation. A-flow and E-flow waveforms in zebrafish hearts can be better identified with the dual mode Doppler technique under the guidance of TD than with the single gate PWD because of the synchronized flow and TD signals. For example, the E-flow within the last heart beat in figure 7*b* may be confused with the another peak in the white circle followed by the end of VOT ejection owing to their similarity of shapes and short separation from A-flow. However, TD shows that Em placed between IVRT and Am can help discriminate E-flow from others. Based on the comparison with the human FD signal, the peak after VOT ejection may be caused by the VOT valve closure; however, further investigations are needed to ascertain this hypothesis.

The performance of dual mode PWD was evaluated by phantom studies. It was shown that dual mode PWD could measure the flow velocity as precisely as single mode PWD. In the phantom study, shown in figure 4, it was found that the velocity ranging from 3 to 15 cm s^{-1} could be measured in Doppler flow mode and that the measured values were close to the pre-set flow speed (p-value $= 0.974$, t-test, double-sided) of the phantom. In figure 6, flow and TD measurements from a moving wire target obtained the same results as the pre-set velocity of 1 mm s^{-1} in the phantom. However, the aliased signal in figure 5*b* could not be recovered by interpolations with neighbouring vectors within the red-dashed line box owing to the decorrelation between the vectors shown in figure 5*d*. To mitigate this problem, the PRF should be increased to avoid saturation caused by aliasing in dual mode PWD. PRF used in this study is limited to 9.5 kHz, which is the maximum PRF of the custom-designed ultrasound imaging system. In the aliased flow signal, caused by squeezing the tube for simulating A-flow, the peak velocity can be estimated by extrapolating the trace shown with the red solid lines in figure 5*b*.

In the longitudinal study of the zebrafish heart with the dual mode PWD, the functional recovery of the amputated heart is investigated. In figure 8*a*, MPI indicating both diastolic and systolic performance sharply decreases at 3 dpa. The decrease of MPI is caused by the shortened IVRT, without significant changes in IVCT shown in figure 8*b*,*c*. This indicates that the ventricular pressure equalizes to the atrium pressure earlier than the normal heart during the early diastolic phase. In addition, the decrease of Em in figure 9*a* indicates the prolongation of ventricular relaxation time, which is interpreted as the increase in stiffness, resulting in slow decrease in ventricular pressure and sharp increase in atrium pressure. Note that the increase of E/Em at 3 dpa, shown in figure 9*e*, indicates that the ventricular filling pressure is increased. Owing to the increased pressure gradient between the heart chambers, the increase of E and the decrease of A result in the increase of the E/A ratio shown in figure 9*d*. Although the increase of E is not statistically significant, the p-value of the paired difference test at 3 dpa approaches the significance level (0.05). Therefore, replicating this experiment with a larger sample size may minimize the measurement errors and subsequently reduce the p-value to achieve statistical significance. These parametric changes in the amputated zebrafish hearts are similar to patterns exhibited in human hearts suffering from diastolic dysfunction of restrictive filling caused by significant reduction in ventricular compliance. All parametric changes indicating dysfunction are recovered to approximately 80–90% within one week, and the diastolic function returns to normal condition after two to three weeks, although previous morphology study indicates that the full recoveries of scars take longer [3].

The standard deviation of peak velocity of A-flow in figure 9*b*, acquired by extrapolation, is relatively larger than the other parameters, whereas f-test (p-value > 0.4) indicates that the standard deviations of other values over all dpa are fairly uniform. Therefore, the errors from extrapolation may be the cause of the larger standard deviation in A-flow compared with those of other parameters that are directly measured.

6. Conclusion

High-frequency dual mode PWD imaging is implemented to acquire flow and TD signals from different positions. The two types of Doppler signals acquired from zebrafish hearts were synchronized in time domain and given in the same heart cycle. In the longitudinal study of functional regenerations of zebrafish hearts, both flow and TD signals were employed to diagnose the diastolic dysfunction of restrictive filling non-invasively. Parametric changes assessed by the dual mode PWD were observed to be in agreement with previous studies using invasive methods, indicating that the functional recovery was mostly accomplished within one week, whereas full recovery from the diastolic dysfunction was exhibited between two to four weeks post-amputation.

Funding statement. This work has been supported by NIH grants RO01-HL79976 and P41-EB002182.

References

1. Bakkers J. 2011 Zebrafish as a model to study cardiac development and human cardiac disease. *Cardiovasc. Res.* **91**, 279–288. (doi:10.1093/cvr/cvr098)
2. Thisse C, Zon LI. 2002 Organogenesis: heart and blood formation from the zebrafish point of view. *Science* **295**, 457–462. (doi:10.1126/science.1063654)
3. Poss KD, Wilson LG, Keating MT. 2002 Heart regeneration in zebrafish. *Science* **298**, 2188–2190. (doi:10.1126/science.1077857)
4. Lien CL, Harrison MR, Tuan TL, Starnes VA. 2012 Heart repair and regeneration: recent insights from zebrafish studies. *Wound Rep. Reg.* **20**, 638–646. (doi:10.1111/j.1524-475X.2012.00814.x)
5. Kikuchi K *et al*. 2010 Primary contribution to zebrafish heart regeneration by gata4(+) cardiomyocytes. *Nature* **464**, 601–605. (doi:10.1038/nature08804)
6. Milan DJ, Jones IL, Ellinor PT, MacRae CA. 2006 *In vivo* recording of adult zebrafish electrocardiogram and assessment of drug-induced QT prolongation. *Am. J. Physiol. Heart Circ. Physiol.* **291**, H269–H273. (doi:10.1152/ajpheart.00960.2005)
7. Ho YL, Shau YW, Tsai HJ, Lin LC, Huang PJ, Hsieh FJ. 2002 Assessment of zebrafish cardiac performance using Doppler echocardiography and power angiography. *Ultrasound Med. Biol.* **28**, 1137–1143. (doi:10.1016/S0301-5629(02)00564-1)
8. Sun L, Xu X, Richard WD, Feng C, Johnson JA, Shung KK. 2008 A high-frame rate duplex ultrasound biomicroscopy for small animal imaging *in vivo*. *IEEE Trans. Biomed. Eng.* **55**, 2039–2049. (doi:10.1109/TBME.2008.919110)
9. Anderson B. 2007 *Echocardiography: the normal examination and echocardiographic measurements*, 2nd edn. Manly, Qld: Australia: MGA Graphics.
10. Nagueh SF *et al*. 2009 Recommendations for the evaluation of left ventricular diastolic function by echocardiography. *J. Am. Soc. Echocardiogr.* **22**, 107–133. (doi:10.1016/j.echo.2008.11.023)
11. Aydin N, Fan L, Evans DH. 1994 Quadrature-to-directional format conversion of Doppler signals using digital methods. *Physiol. Meas.* **15**, 181–199. (doi:10.1088/0967-3334/15/2/007)
12. Jensen JA. 1996 *Estimation of blood velocities using ultrasound: a signal processing approach*. New York, NY: Cambridge University Press.
13. Hu C, Zhang L, Cannata JM, Yen J, Shung KK. 2011 Development of a 64 channel ultrasonic high frequency linear array imaging system. *Ultrasonics* **51**, 953–959. (doi:10.1016/j.ultras.2011.05.010)
14. Cannata JM, Williams JA, Zhang L, Hu CH, Shung KK. 2011 A high-frequency linear ultrasonic array utilizing an interdigitally bonded 2–2 piezo-composite. *IEEE Trans. Ultrason. Ferroelectr. Freq. Control* **58**, 2202–2212. (doi:10.1109/TUFFC.2011.2070)
15. Tei C, Ling LH, Hodge DO, Bailey KR, Oh JK, Rodeheffer RJ, Tajik AJ, Seward JB. 1995 New index of combined systolic and diastolic myocardial performance: a simple and reproducible measure of cardiac function: a study in normals and dilated cardiomyopathy. *J. Cardiol.* **26**, 357–366.